FRIEDRICH-SCHILLER-UNIVERSITÄT JENA

Trapezoidal Wave

by interference of Goodwin oscillators

for the module molecular algorithms

supervised by Dr. -Ing habil. Hinze

written by Lasse Steinhoff

July 27, 2026

Contents

1 Introduction

Nonlinear dynamical systems can exhibit several qualitatively different behaviors depending on their parameters. Besides converging to a stable steady state or diverging without bound, many systems undergo a Hopf bifurcation, which gives rise to self-sustained limit-cycle oscillations. Such oscillatory behavior provides a foundation for engineering dynamic chemical reaction networks capable of generating periodic signals. Rather than producing a simple sinusoidal oscillation, the objective of this work is to design a chemical reaction network whose steady state oscillations approximate a trapezoidal waveform. Achieving such a complex periodic output requires the coordinated superposition of multiple oscillatory components with well-defined amplitudes, frequencies, and phase relationships. For a trapezoidal waveform, the first five odd harmonics of the truncated Fourier series of a square wave were chosen as target sinusoids (Figure 1).

$$f(t) = \sum_{i=1,3,5,\ldots}^{\infty} \frac{\sin(it)}{i}$$

$$f_5(t) = \sin(t) + \frac{\sin(3t)}{3} + \frac{\sin(5t)}{5} + \frac{\sin(7t)}{7} + \frac{\sin(9t)}{9} \tag{1}$$

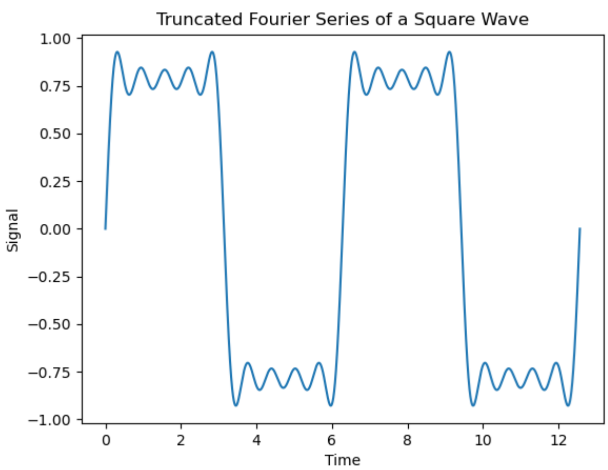

Figure 1: First five odd harmonics of the truncated Fourier series of a square wave.

1.1 Architecture

The final reaction network consists of five independently optimized Goodwin oscillators whose state variables X_i represent the first five odd harmonics of the truncated Fourier series. The mean-centered variables X_i are summed to form the superposition S, which is low-pass filtered through a cascade of intermediate variables C. The reaction rate constant k determines the filter strength, resulting in the trapezoidal output T.

$$S = \sum_{i=1}^{5} (X_i - \overline{X_i})$$
$$\frac{dC_3}{dt} = k(O - C_3)$$
$$\frac{dC_2}{dt} = k(C_3 - C_2)$$
$$\frac{dC_1}{dt} = k(C_2 - C_1)$$
$$\frac{dT}{dt} = k(C_1 - T)$$

1.2 Goodwin Oscillator

The Goodwin oscillator is a three variable differential equation model representing a gene regulatory network. It describes the production of mRNA X, protein Y, and a regulatory product Z that inhibits its own synthesis through negative feedback. This delayed negative feedback is a common mechanism responsible for sustained oscillations in biological systems. The repression is modeled with a Hill equation which provides the nonlinearity necessary for the emergence of stable limit cycle oscillations. β are the production rates, γ are the decaying rates, and n is the Hill coefficient. The half saturation constant was fixed at one for simplicity.

$$\frac{dX}{dt} = \frac{\beta_X}{1 + Z^n} - \gamma_X X$$
$$\frac{dY}{dt} = \beta_Y X - \gamma_Y Y$$
$$\frac{dZ}{dt} = \beta_Z Y - \gamma_Z Z$$

Figure 2 illustrates the chemical reaction network of a Goodwin oscillator. The state variables are represented as molecular species, whereas the production and degradation processes are represented by chemical reactions.

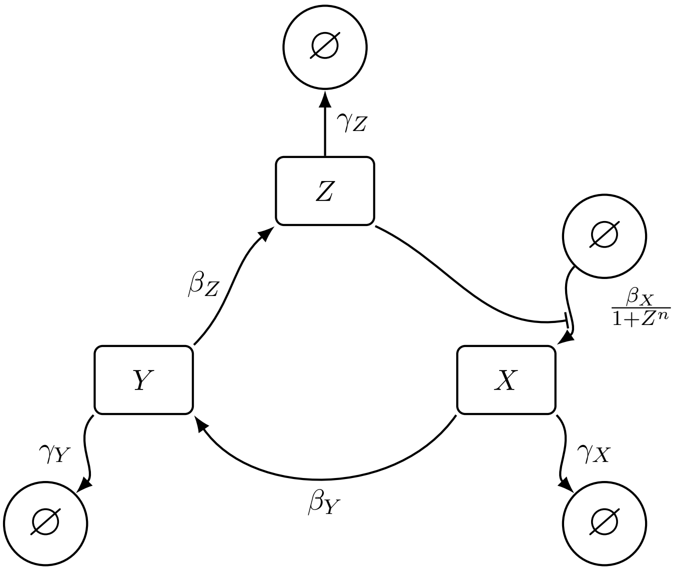

Figure 2: Chemical reaction network representation of a Goodwin oscillator. The state variable X promotes the production of Y with rate β_Y, which promotes the production of Z with rate β_Z. Z represses the production of X with rate β_X through a negative feedback with Hill coefficient n. All state variables are degraded to $\varnothing$ with the corresponding degradation rates γ_X, γ_Y, and γ_Z.

In order to determine the parameters required for each oscillator to generate the desired amplitude and frequency, an optimization procedure identifies suitable Goodwin parameter sets. At first, randomly generated parameter sets are screened for the existence of sustained oscillations by evaluating the Jacobian at steady state. These candidates are then numerically integrated and analyzed using a Fast Fourier transform to determine their dominant angular frequency, oscillation amplitude, and spectral purity. Finally, a mutation algorithm iteratively adjusts production rates (β_X, β_Y, β_Z) and degradation rates (γ_X, γ_Y, γ_Z) according to the relative deviations from the target amplitude and frequency.

2 Materials and Methods

2.1 Hopf Bifurcation

A Hopf bifurcation marks the transition from a stable steady state to sustained oscillations. It occurs when the largest real part of a complex conjugate pair of Jacobian eigenvalues changes sign. To locate the bifurcation point, a single parameter was varied until two parameter values were identified for which the largest real part of the eigenvalues had opposite signs. The midpoint of this interval was then used to adjust the parameter to a value near the Hopf bifurcation point. For each randomly generated parameter set, the steady state was obtained by numerically solving

$$\gamma_X \gamma_Y \gamma_Z \, Z(1 + Z^n) = \beta_X \beta_Y \beta_Z,$$

using the root scalar function from the SciPy library. The Jacobian matrix was then evaluated at the steady state

$$J(X, Y, Z) = \begin{bmatrix} -\gamma_X & 0 & -\dfrac{\beta_X n Z^{n-1}}{(1 + Z^n)^2} \\ \beta_Y & -\gamma_Y & 0 \\ 0 & \beta_Z & -\gamma_Z \end{bmatrix},$$

and its eigenvalues were computed numerically using NumPy.

2.2 Fourier Analysis

Starting from an initial parameter set, the oscillator was integrated using SciPy. To eliminate transient dynamics, the initial part of the simulated time series was discarded before its oscillation amplitude, dominant angular frequency, and spectral purity were determined using a Fast Fourier Transform (FFT) implemented in NumPy. The amplitudes were normalized as

$$\frac{2|\mathrm{FFT(X)}|}{N},$$

where N denotes the number of sampled data points. The dominant oscillation frequency was identified as the frequency corresponding to the largest non zero Fourier amplitude, which was converted to angular frequency by

$$\omega = 2\pi f.$$

In addition, sinusoidal purity was quantified as the ratio of the dominant Fourier amplitude to the sum of all non zero Fourier amplitudes, providing a measure of how closely the oscillation resembled a pure sinusoidal waveform.

2.3 Mutation Algorithm

The quality of each candidate solution was quantified using a fitness score that combines spectral purity P with penalties for the relative amplitude A and angular frequency ω errors.

$$S = P - \left(\frac{A - A_{\text{target}}}{A_{\text{target}}}\right)^2 - 1000\left(\frac{\omega - \omega_{\text{target}}}{\omega_{\text{target}}}\right)^2 \quad (2)$$

Since accurate frequency matching is essential for harmonic reconstruction, the relative frequency error was weighted by a factor of 1000. Relative errors were squared to penalize larger deviations more strongly. As the optimized amplitude and angular frequency approach their target values, the relative errors converge to zero. Because the spectral purity is bounded between 0 and 1, the score approaches its maximum value of 1. The evaluation of all mutated parameter vectors was parallelized, as each candidate can be simulated independently. The assignment of production and degradation rates to amplitude and frequency optimization was guided by heuristic considerations. If the oscillator amplitude was below the target, the production rates increased, while they decreased when the amplitude exceeded the target. Similarly, when the oscillation frequency was below the target, the degradation rates increased, while they decreased when the frequency exceeded the target. The highest scoring parameter set was retained and used as the basis for the next iteration until no further improvement was obtained or the optimization reached its stopping criterion.

2.4 Phase Alignment

One of the main challenges in reconstructing the target waveform is identifying a time interval during which the individual Goodwin oscillators are sufficiently in phase. Although each oscillator could be optimized to reproduce the target frequency and amplitude with high spectral purity, slight deviations in their frequencies and initial phases caused their superposition to vary continuously over time. Consequently, no single time point guaranteed an optimal reconstruction. To identify the interval in which the oscillators were most closely synchronized, the coupled oscillator system was simulated over a sufficiently long time span. The sliding window corresponding to one period of the fundamental harmonic was used to calculate the mean squared error (MSE) between the superposition S and the analytical target waveform (Equation 1). The interval yielding the lowest MSE was selected for visualization.

3 Result

The properties of the identified Goodwin oscillators in Equation 1 are listed in Tables 1 and 2. The optimized amplitudes had a smallest deviation of 0.1% with the seventh harmonic, and the largest deviation was the first harmonic with 9.4%. The angular frequencies closely match their target values, although the seventh harmonic shows the largest deviation of 1.16%.

Harmonic	Amplitude	Amplitude Deviation (%)	ω (rad/s)	ω Deviation (%)
1	1.094	9.4	6.282	0.02
3	0.347	4.1	18.846	0.02
5	0.209	4.5	31.535	0.38
7	0.143	0.1	43.471	1.16
9	0.117	5.3	56.537	0.02

Table 1: Accuracy of the optimized Goodwin oscillators. Relative deviations are calculated with respect to the target amplitude ($1/i$) and target angular frequency ($2\pi i$).

Since both the score and the purity have an upper bound of 1.0, the achieved scores above 0.88 and the purities above 0.899 indicate that the optimization successfully identified parameter sets with high agreement with the target harmonics.

Harmonic	Score	Purity	Mean
1	0.916	0.925	3.818
3	0.897	0.899	2.153
5	0.884	0.920	0.844
7	0.905	0.918	0.236
9	0.921	0.944	0.278

Table 2: Score, purity, and mean of the optimized Goodwin oscillators.

Figure 3 shows the interval $t \in [96892, 96893]$ with the lowest MSE of 0.005571, and compares the mean-centered and summed superposition S with the ideal analytical target waveform (Equation 1). The trapezoidal waveform T was filtered by applying $k = 55$.

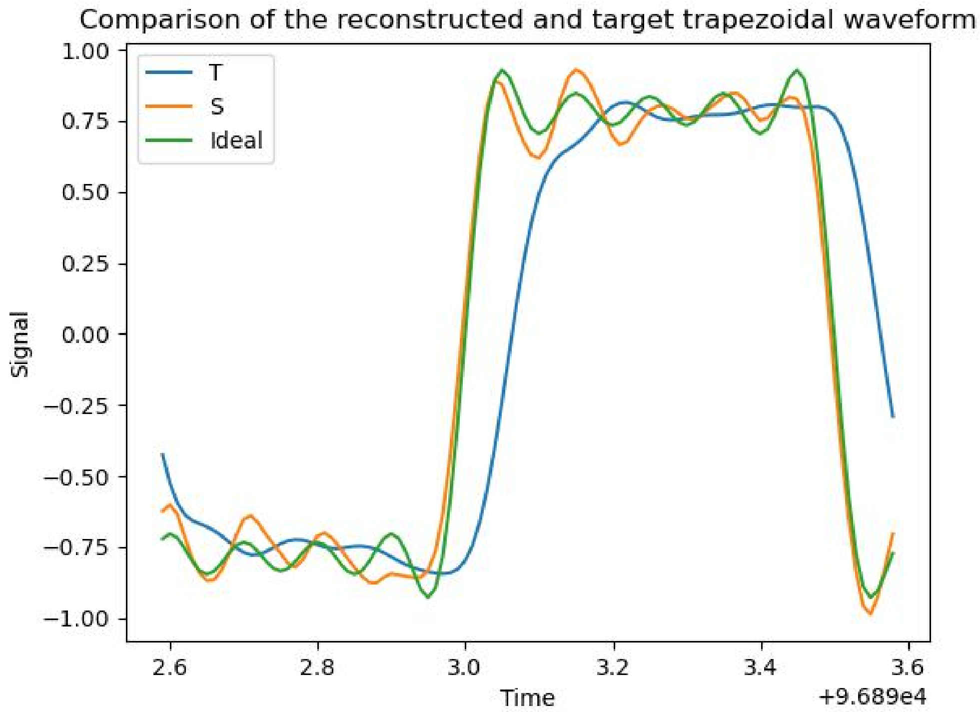

Figure 3: Comparison of mean-centered and summed output of the oscillators S (orange), the ideal target waveform (green), and the low-pass filtered output T (blue) with $k = 55$ for the time interval $t \in [96892, 96893]$.

Figure 4 shows the long-term behavior of the reconstructed waveform over an extended simulation period with the best interval occurring in the middle. The oscillation remains stable throughout the simulation, while its amplitude varies slowly over time.

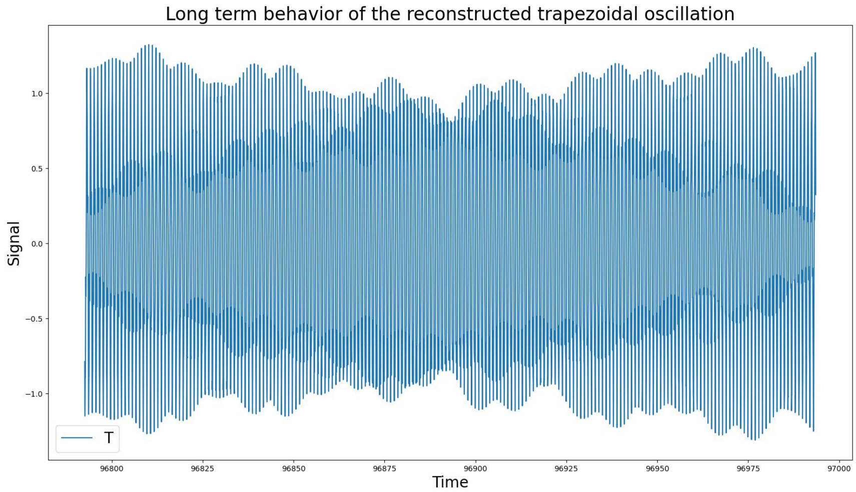

Figure 4: Long-term behavior of the low-pass filtered output T for $k = 55$ over the time interval $t \in [96792, 96993]$.

4 Discussion

The main limitation of the reconstruction is that the optimized oscillator frequencies cannot be matched exactly using the current optimization strategy. Therefore, the relative phases periodically move into and out of alignment, resulting in long-term amplitude variations. In addition to phase drift, the remaining spectral impurity of approximately 10% also contributed to deviations in the reconstructed amplitudes. A more fundamental solution would be to identify initial conditions that place each oscillator at the desired position on its limit cycle, thereby establishing the required phase relationship from the beginning of the simulation. Consequently, long-term phase drift would still arise from frequency mismatches. Increasing the penalty assigned to the relative ω error in the fitness function (Equation 2) could reduce these deviations, allowing the reconstructed trapezoidal waveform to remain stable over substantially longer simulation times. The mutation heuristic is based on the assumption that production rates predominantly control oscillation amplitude, whereas degradation rates mainly determine oscillation frequency. However, this simplification neglects the strong nonlinear coupling between all parameters in the Goodwin oscillator. In reality, changes in a single parameter often affect both amplitude and frequency simultaneously. Another possible optimization strategy would be to separate the optimization into two consecutive stages. The first stage should exclusively optimize the angular frequency and spectral purity. Once the desired frequency has been achieved with sufficient accuracy, the second stage could refine the oscillation amplitude while constraining the frequency to remain close to its optimized value. An alternative approach would be to identify a single oscillator whose oscillatory dynamics already contain the first five harmonic components. Because all harmonics would originate from the same limit cycle, this approach could eliminate the beating observed in the present implementation. Additional refinement with larger numbers of mutated parameter sets did not improve the fitness score, indicating that the current optimization strategy had converged to an apparent local optimum. Nevertheless, the optimized oscillators reproduce the target harmonics with high frequency accuracy and spectral purity, demonstrating the feasibility of the approach. This work illustrates how concepts from nonlinear dynamical systems and classical signal processing can be combined to engineer a predefined oscillatory behavior. Although additional improvements are required to achieve fully autonomous synchronization, the presented approach provides a proof of principle that relatively simple gene regulatory oscillators can be organized into larger functional systems capable of generating predefined temporal patterns.

A Optimized Goodwin Oscillator Parameters

Table 3: Optimized parameter sets of the five Goodwin oscillators used for trapezoidal waveform reconstruction.

Harmonic	β_X	β_Y	β_Z	γ_X	γ_Y	γ_Z	n
1	34.205	2.625	1.140	4.149	3.809	2.967	16
3	17.435	23.010	4.039	5.253	18.013	11.384	38
5	42.542	5.618	33.481	20.823	4.343	36.102	31
7	14.529	42.593	49.597	30.000	30.000	16.560	26
9	24.131	39.155	54.834	37.680	10.008	58.906	28